Original Paper

Development of a Small-scale Supersonic Flight Experiment Vehicle as a Flying Test Bed for Future Space Transportation Research

By Kazuhide MIZOBATA, Ryojiro MINATO, Ken HIGUCHI, Masazumi UEBA, Syohei TAKAGI,
Daisuke NAKATA, Kazuyuki HIGASHINO and Nobuhiro TANATSUGU

Aerospace Plane Research Center (APReC), Muroran Institute of Technology, Muroran, Japan

Innovation in technologies for high-speed atmospheric flights is essential for establishment of both supersonic/hypersonic and reusable space transportations. It is quite effective to verify such technologies through small-scale flight tests in practical high-speed environments, prior to installation to large-scale vehicles. Thus we are developing a small-scale supersonic flight experiment vehicle as a flying test bed. Several aerodynamic configurations are proposed and analyzed by wind tunnel tests. A twin-engine configuration with a cranked-arrow main wing is selected as the baseline of the first generation vehicle. Its flight capability is predicted by point mass analysis on the basis of aerodynamic characterization and propulsion performance estimation. In addition, a prototype vehicle with an almost equivalent configuration and dimension is designed and fabricated for verification of the subsonic flight characteristics of the experiment vehicle. Its first flight test is carried out and good flight capability is demonstrated. Furthermore a revised aerodynamic configuration with an air-turbo ramjet gas-generator cycle (ATR-GG) engine is being designed for the second generation design with improvement in flight capability at higher Mach numbers. Development of the engine, airframe structure, and autonomous guidance/control system is underway. This prospective flight experiment vehicle will be applied to flight verification of innovative fundamental technologies for high-speed atmospheric flights such as turbo-ramjet propulsion with endothermic or biomass fuels, MEMS and morphing techniques for aerodynamic control, aero-servo-elastic technologies, etc.

Key Words: Space Transportation, Flying Test Bed, Flight Test, Supersonic, Jet Propulsion

Nomenclature and Abbreviations

AOA	:	angle of attack
b	:	wing span
C_D	:	drag coefficient
C_L	:	lift coefficient
C_l	:	rolling moment coefficient
C_m	:	pitching moment coefficient
C_n	:	yawing moment coefficient
CG	:	center of gravity
M	:	flight or flow Mach number
MAC	:	mean aerodynamic chord
p	:	pressure or angular rate of rolling motion
V	:	flight airspeed
α	:	angle of attack
β	:	side slip angle
δ	:	deflection angle of elevator
δ_a	:	deflection angle of aileron
δ_r	:	deflection angle of rudder
ψ	:	yaw angle

1. Introduction

Innovation in technologies for high-speed atmospheric flights is essential for establishment of supersonic/hypersonic and reusable space transportations. It is quite effective to verify such technologies through small-scale flight tests repeatedly in practical high-speed environments prior to installation to large-scale vehicles. Thus we are developing a small-scale supersonic flight experiment vehicle as a flying test bed.

We propose several candidate vehicle configurations and characterize their aerodynamics through wind tunnel tests. On the basis of their results, a twin engine configuration with a cranked-arrow main wing is selected as the baseline. Generally, the cranked-arrow wing has good aerodynamic characteristics over a wide range of flight Mach number and angle of attack, because of its stable vortex system. Such aerodynamics have been investigated in detail for wing-fuselage configurations without tails by Rinoie, Kwak, et al.[1-5] But those for overall configuration of practical vehicles with tails and control surfaces have not yet been clarified sufficiently. Then the aerodynamic stability and controllability for the proposed baseline configuration are analyzed through wind tunnel tests in this development study. These treatments and results will be elaborated in Section 2.

On the other hand, a counter-rotating axial fan turbojet (CRAFT) engine is proposed for propulsion for this vehicle. Its concept and design will be outlined briefly in Section 3. On the basis of the aerodynamic characterization and propulsion design analysis, flight capability prediction is carried out by point mass analysis

of motion. It will be described in Section 4. Prior to the construction of the supersonic vehicle, a prototype is designed and fabricated in order to verify the subsonic flying characteristics of the vehicle configuration through flight tests. Section 5 will outline the design of the prototype vehicle and its maiden flight test carried out in August 2010. A revised aerodynamic configuration with an air-turbo ramjet gas-generator cycle (ATR-GG) engine will be proposed and its aerodynamics and flight capability will be assessed in Section 6. Then Section 7 is conclusions.

2. Configuration Designs and Aerodynamic Characterization

2.l. Proposed configuration designs

Five configurations shown in Fig. l were proposed. Their concepts are as follows:

➢ M2005: a single engine is installed in the fuselage and an intake is located at the nose, in order to minimize the projected front area and to place the thrust vector nearest to the fuselage axis. These would minimize parasite and trim drags.

➢ M2006: Twin engines are installed underneath the main wing at the both sides of the fuselage in order to attain sufficient acceleration and ascent capability. A diamond wing section of 6% thickness is adopted for reduction of wave drag during supersonic flights. Its main wing has a cranked-arrow planform for stable aerodynamic characteristics. A high-wing configuration with a dihedral of 1.0 degree is also adopted in order to attain sufficient roll stability.

➢ K2005: A single engine is installed at the root of the vertical tail on the rear part of the fuselage. The main wing has a variable planform with sweep-back angles of 30 and 50 degrees. A canard is adopted instead of a horizontal tail.

➢ K2006: A slight extent of blended-wing-and-body feature is added to K2005; the connecting portions between the wings, the fuselage, and the engine nacelle are smoothed. This would reduce wing-body interference drag.

➢ O2006: A single engine is installed in the fuselage and two intakes are located on the both sides of the fuselage. A so-called close-coupled canard is equipped for enhancement of lift during subsonic flights.

On the basis of wind tunnel tests and engine performance prediction, the thrust margin, i.e. thrust minus parasite drag, was analyzed for various sets of flight Mach number and altitude. An optimistic assessment of attainability of supersonic flight was carried out using the thrust margin map where the aspect of fuel consumption was neglected. As a results of this analysis,

the twin engine configuration M2006 was found to be the only one capable of attaining supersonic flights. Thus M2006 was selected as the baseline configuration. Its overall shape and dimensions are illustrated in Fig.2. It has ailerons, a rudder, and all-pivoting horizontal tails as control surfaces.

In addition, a modified configuration M2006prototype was proposed for construction of a prototype vehicle, in which the following modifications were adopted as shown in Fig.3:

(a) Its horizontal and vertical tails are enlarged and less swept-back for enhancement of stability and controllability during takeoff and landing.

(b) Its lateral control capability is enhanced by adopting all-pivoting elevons.

(c) A pair of inboard flaps is installed for takeoff and landing.

(d) Its engine nacelles are connected to the fuselage on its both sides for the sake of convenience in fabrication and maintenance.

(e) Its nose is extended forward in order to attain sufficient capacity for installing fuel and avionics in the fuselage.

Series of wind tunnel tests were carried out for these configurations M2006 and M2006prototype. The results will be outlined in the following subsections.

(a) M2005   (b) M2006

(c) K2005

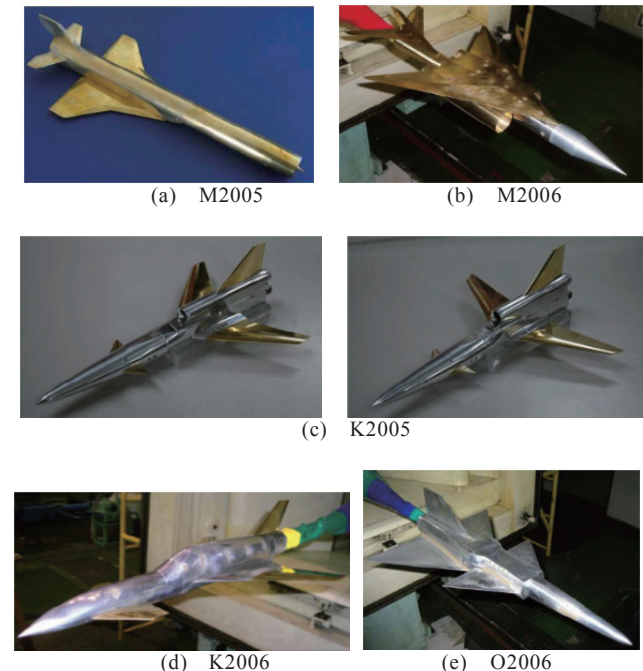(d) K2006   (e) O2006

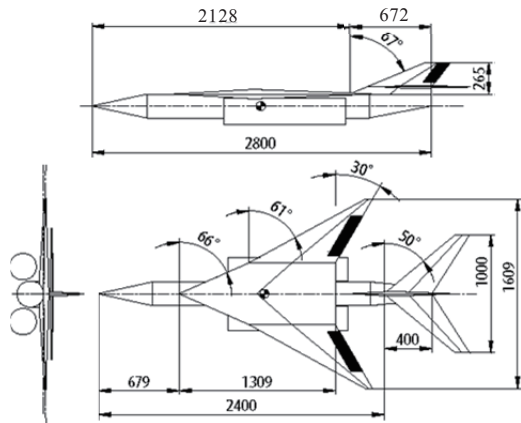Fig. 1. Proposed aerodynamic configurations.

Fig. 2. The baseline configuration M2006. It has all-pivoting horizontal tails.
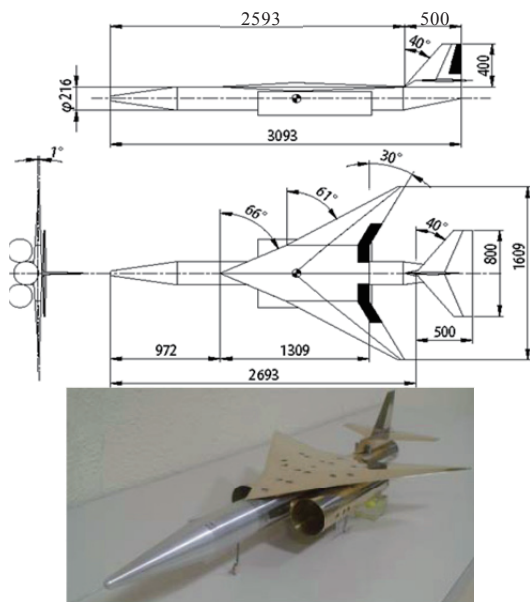

Fig. 3. The modified configuration M2006prototype for constructing a prototype vehicle.
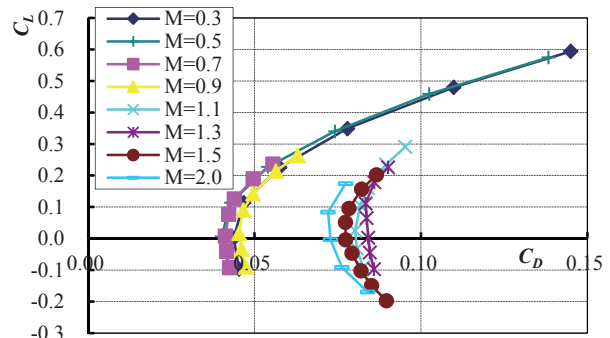
2.2. Lift and drag characteristics

The Comprehensive High-speed Flow Test Facility at the Institute of Space and Astronautical Science (ISAS) of the Japan Aerospace Exploration Agency (JAXA) was used for the present aerodynamic characterization. The facility consists of a transonic wind tunnel for Mach 0.3 to 1.3 and a supersonic wind tunnel for Mach 1.5 to 4.0. The cross-sectional size of their test sections is 600x600mm. The results for lift and drag are shown in Fig. 4. The maximum value of the angle of attack (AOA) is 10 degrees for subsonic conditions and 4 degrees for transonic/supersonic conditions. These small values are correspondent to the force capacity of the internal balance utilized. The lift coefficient curves show quite a good linearity with a slope of 0.058/deg. for subsonic, 0.065/deg. for transonic, and 0.043/deg. for supersonic regime, where the elevators are fixed. The so-called sound barrier, i.e. the drag peak at transonic regime, is small owing to the large sweep-back angles of the wing and tails. Concerning the configuration M2006prototype, additional

subsonic wind tunnel tests were carried out at Osaka Prefecture University. Their results are shown in Fig. 5 for AOA ranging from -30 to +30 deg. The linearity of its lift coefficient is found to be good for this wide range of positive AOA, owing to the stability of the vortex system over the present cranked-arrow wing with a large inboard sweepback angle of 66deg[1]. The linearity deteriorates for negative AOA probably because the engine nacelles would interfere with the vortex system.
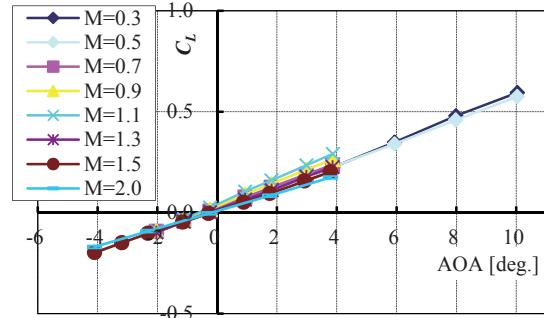
(a) Lift coefficient versus angle of attack.

(b) Drag polar.
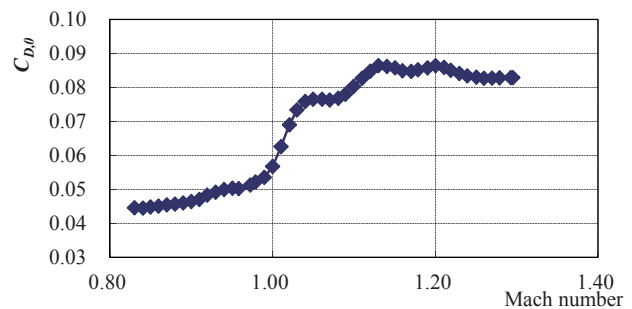
(c) Mach number dependence of the zero-lift drag coefficient at a zero angle of attack.
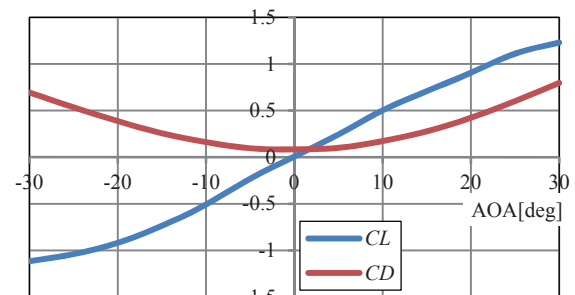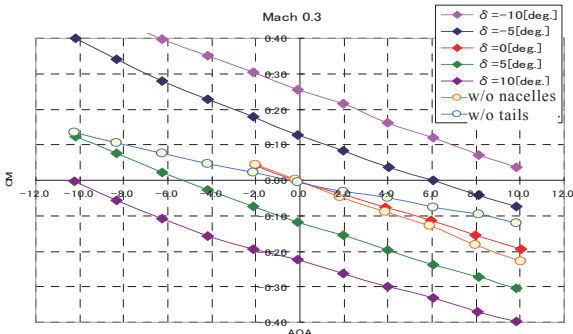Fig. 4. Lift and drag characteristics of the baseline configuration M2006.

Fig. 5. Subsonic lift and drag characteristics of the modified configuration M2006prototype.
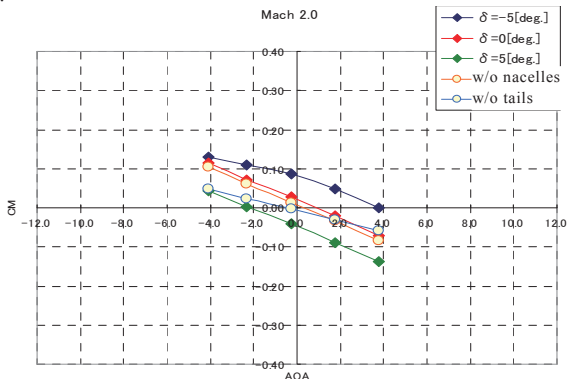
2.3. Trim capability for pitching motion

The measured variation of the pitching moment coefficient C_m with varying AOA is shown in Fig. 6 (a) and (b) for a center of gravity (CG) location of 20% of the mean aerodynamic chord (MAC) and for several elevator deflection angles ranging from -10 to +10 degrees. Note that the elevator deflection measures positive when the trailing edge of the elevator deflects downwards. The negative gradients of the curves indicate static stability in the pitching motion. The value of the gradient, i.e. the extent of the stability, varies in accordance with the CG location; the more forward the CG lies, the larger the stability is. On the other hand, the intercepts on the horizontal AOA axis represent the trim conditions. For example, at Mach 0.3 the vehicle can attain pitch trim at AOA of 6.0 deg. with an elevator deflection of -5 deg. for a CG location of 20%MAC.
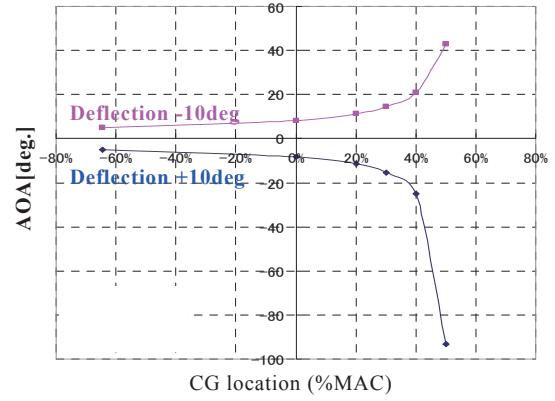
Fig. 6 (c) shows the pitch trim capability for various CG locations, where the upper magenta curve indicates the AOA for pitch trim at each CG location for an elevator deflection of -10 deg. and the lower blue curve for an elevator deflection of +10 deg. So the difference in AOA between the two curves is the range where pitch trim can be attained. The more forward the CG is located, the narrower the AOA range for pitch trim is, and vice versa. Note that the more backward CG location than 40%MAC is shown to cause pitching instability. A CG location of 25 to 30%MAC is found to be appropriate for both the pitch trim capability and stability.
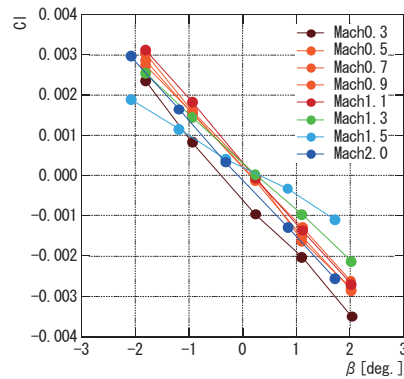

(c) Pitch trim capability at Mach 0.3.

Fig. 6. Pitching moment characteristics measured by wind tunnel tests.
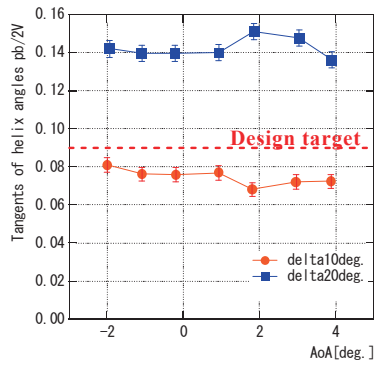
2.4. Trim and control capability for rolling motion

Fig. 7 (a) shows the measured rolling moment coefficient C_l versus the side slip angle β for several Mach numbers. The static roll stability is indicated by the negative gradients of the curves for all of the Mach numbers. For assessment of the roll control capability, the tangent of helix angle $pb/2V$ is a convenient measure, where p is the angular rate of the rolling motion, b is the wing span, and V is the airspeed. This helix angle means the angle at which the main wing tips draw a pair of helixes during a rolling maneuver. It depends theoretically only on aircraft's geometry and is independent of dimension, airspeed and angle of attack. It can be estimated from wind tunnel test data using the following equation[6]:

$$\frac{pb}{2V} = \frac{C_{l,\delta_a}\delta_a K}{2C_{l,p}} \qquad (1)$$

where the roll damping derivative C_{lp}, and the correction factor for large aileron deflections K are empirical factors [6]. Its values evaluated from the present wind tunnel tests are shown in Fig. 7 (b) for aileron deflections of 10 and 20 degrees. The dotted red line indicates a design target for acrobatic/fighter aircraft. Thus sufficient roll control capability is predicted for the present M2006 configuration.

(a) Pitching moment coefficient versus angle of attack for several elevator deflections with a CG location of 20%MAC and at Mach 0.3.

(b) Pitching moment coefficient versus angle of attack for several elevator deflections with a CG location of 20%MAC and at Mach 2.0.

(a) Rolling moment coefficient versus side slip angle for several Mach numbers ranging from 0.3 to 2.0.

(b) Estimated tangent of helix angle main wing tips draw at Mach 0.7.

Fig. 7. Rolling moment characteristics measured by wind tunnel tests.

2.5. Trim and control capability for yawing motion

Fig. 8 (a) shows the measured yawing moment coefficient C_n versus the yaw angle ψ for several Mach numbers. The static yaw stability is indicated by the negative gradients of the curves for all of the Mach numbers. Fig. 8 (b) shows the yaw trim capability. The intercepts on the horizontal axis represent the trim conditions. Thus yaw trim can be attained at yaw angles of -8 or -16 deg. with rudder deflections of 10 or 20 deg., respectively. The rudder power C_{n,δ_r} evaluated from the present wind tunnel tests is shown in Fig. 8 (c) where the dotted red line is a design target. Thus sufficient rudder effectiveness is predicted for the present M2006 configuration.
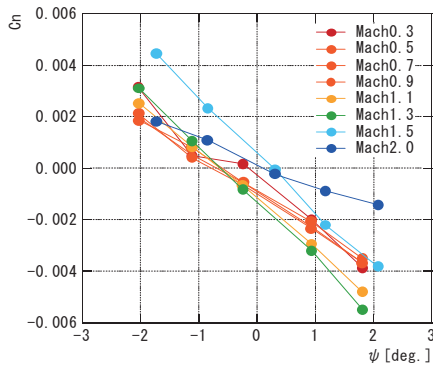
(a) Yawing moment coefficient versus yaw angle for several Mach numbers ranging from 0.3 to 2.0.
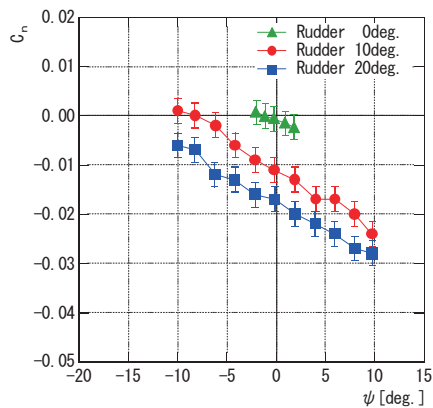
(b) Yawing moment coefficient versus yaw angle for some rudder deflections at Mach 0.7.
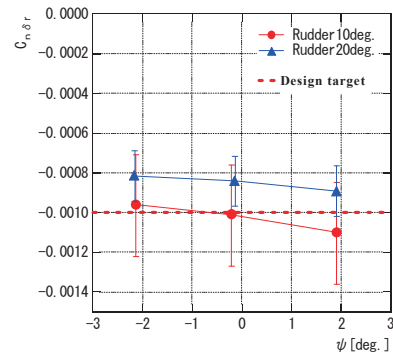

(c) Rudder power for some rudder deflections.

Fig. 8. Yawing moment characteristics measured by wind tunnel tests.

3. Concept and Design of the Proposed Engine

A counter-rotating axial fan turbojet (CRAFT) engine was proposed and designed preliminarily for installation onto the proposed supersonic flight experiment vehicle [7-9]. In this engine the rotor fans in the first and the second stages rotate in an opposite direction and the stator fans can be eliminated to establish a compactness of the engine configuration. Its thrust and specific impulse evaluated for an afterburner fuel/air ratio of 0.025 by a thermodynamic cycle analysis are shown in Fig. 9. The operational upper boundary in terms of flight Mach number is correspondent to the constraint on the turbine inlet temperature (TIT). For more practical design of the engine components, CFD analysis has been carried out using the turbo-machinery analysis software FineTURBO as illustrated in Fig. 10. A set of prototype counter-rotating fans was fabricated and is undergoing ground rig tests as shown in Fig. 11.
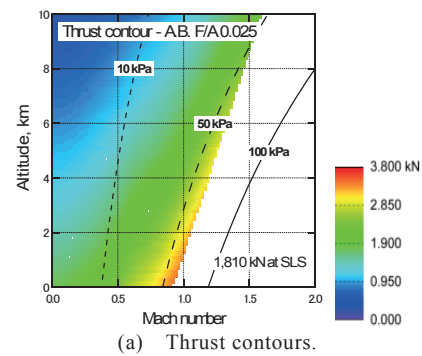
(a) Thrust contours.
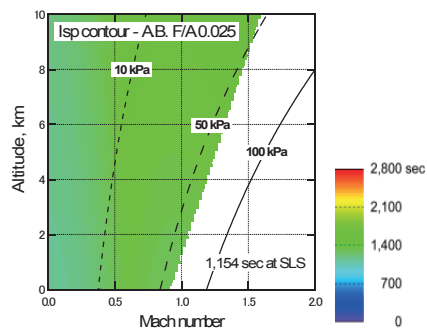
(b) Specific impulse contours.

Fig. 9. Predicted performance of the proposed counter-rotating axial fan turbojet (CRAFT) engine at an afterburner fuel/air ratio of 0.025.
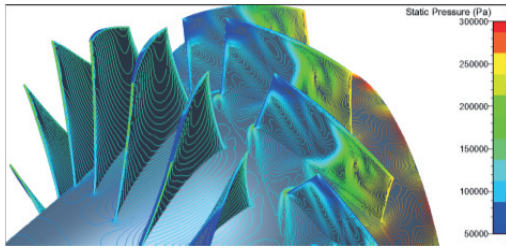
Fig. 10.   CFD analysis of counter-rotating axial fans for the proposed turbojet engine.


Fig. 11.   The fabricated first-stage fan in the prototype counter-rotating axial fan turbojet (CRAFT) engine and its ground test facility.

4.   Flight Capability Prediction

Flight capability of the proposed supersonic experiment vehicle was predicted by point mass analysis on the basis of the lift and drag characteristics measured by wind tunnel tests, thrust and specific impulse evaluations of the proposed engine, and a preliminary weight estimation of the airframe. One of the results is shown in Fig. 12, where three flight trajectories with return cruise at altitudes of 10, 12, and 14 km are illustrated. It is found that the vehicle can attain supersonic flight at Mach 1.6 for about one minute and a sufficient endurance for return flight. The upper limit in flight Mach number is correspondent to that in the turbine inlet temperature of the proposed engine design. This constraint can be eliminated in the proposed revision engine, i.e. an air-turbo ramjet gas-generator cycle (ATR-GG) engine.
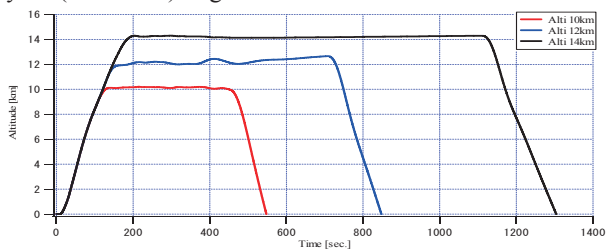
(a) The history of altitude.
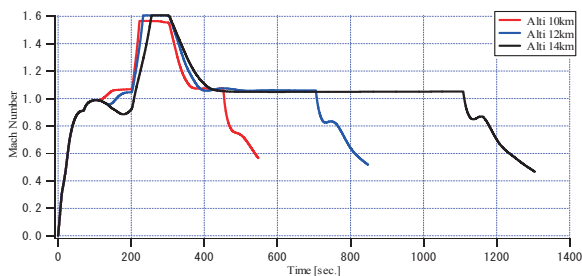
(b) The history of flight Mach number.
Fig. 12.   One of the results of the flight capability analysis.

5.   A Prototype Vehicle for Subsonic Flight Tests

5.1 Configuration design and fabrication

Prior to construction of the supersonic vehicle, a prototype with the modified configuration M2006prototype was designed and fabricated in order to verify the subsonic flying characteristics of the vehicle configuration through flight tests. Its overall appearance is shown in Fig. 13.   It has semi-monocoque structure composed of spars, stringers, and skins made of CFRP and ribs and ring frames made of wood. The forward part of its fuselage is made of GFRP so as to install antennas inside. Its empty mass is 22.2kg including a propulsion system. The maximum fuel mass is 4.6kg, and the avionics system is 0.2kg. Then the total takeoff mass is 27.0kg. The propulsion system is model-scale twin turbojet engines available on the market. Their rated total thrust is 330N at a sea-level static condition and the maximum airspeed for level flight of the vehicle is predicted to be 104m/sec according to the wind-tunnel test data. Its nickname is OHWASHI (Steller's Sea Eagle) which was selected by an advertised prize contest.

(a) The airframe before painting.

(b) The painted and fully equipped vehicle (without a Pitot boom).
Fig. 13.   Overall appearance of the fabricated prototype vehicle.

5.2.   On-board measurement system

For onboard data acquisition, the following measurement units were installed in the fuselage:

➢ A combined GPS/INS navigation recorder which acquires and records GPS positioning data and accelerations and rotation rates with respect to body-fixed axes.

➢ An air data sensor (ADS) including a 5-hole Pitot tube, which measures the dynamic pressure as well as the differential pressure between the pair of pressure ports aligned in the vertical or lateral plane of symmetry on the conical nose of the Pitot boom. Correlation between the measured differential pressure $\Delta p_{vertical}$ or $\Delta p_{lateral}$ and angle of attack α or side slip angle β is described by the equations

$$\frac{\Delta p_{vertical}}{p_{dyn}} = f_1(\alpha), \quad \frac{\Delta p_{lateral}}{p_{dyn}} = f_2(\beta) \qquad (2).$$

where p_{dyn} is the measured dynamic pressure. The

correlation functions f_1 and f_2 were determined as fourth order polynomials by wind tunnel tests for angle of attack α or side slip angle β ranging from -20 to +20 degrees. The so-called position error caused by rotation of the vehicle is estimated and compensated using the angular rates measured with the INS unit.

➢ A control signal detector which detects the control signals for servo-motors of control surfaces and throttle.

➢ A pair of electric control units for the twin turbojet engines which record throttling signals and rotations of the engines.

➢ A small video camera which records outside view.

5.3. First flight test

The first flight test of the prototype vehicle was carried out in August 2010 at the Shiraoi Airfield nearest to Muroran Institute of Technology. The length of the runway is 800m. The vehicle was radio-controlled by a pilot on the ground. A snapshot of the preflight check on the onboard avionics is shown in Fig. 14. The appearance of the prototype vehicle ascending just after takeoff is shown in Fig. 15. Its flight trajectory is illustrated in Fig. 16 on the basis of the onboard GPS data. The vehicle circled six times above and around the runway for 4 minutes and a half. Its flight stability and controllability were quite adequate. The airspeed and angles of attack and sideslip estimated from the ADS data show twelve high-speed flights and twelve low-speed turns with pitch-up attitudes and right sideslips, in accordance with the six rounds, as shown in Fig. 17. The maximum air speed 58m/sec is considerably smaller than prediction due to drag enhancement described below.

Because control inputs for the control surfaces and engine throttle were quite frequent in the flight test, local-quasi-steady data were extracted from the overall data acquired. Aerodynamic coefficients were estimated from the acceleration and angular rates so extracted and the thrust characteristics measured by ground tests. The results for lift and drag coefficients in quasi pitch-trim conditions are shown in Fig. 18 in comparison with wind tunnel data. The lift coefficients from the flight test agree quite well with those from wind tunnel tests. Note that the lift curve slope in the pitch-trim condition is smaller than that in fixed-elevator condition since a downward lift on the horizontal tail is required for pitch trim. On the other hand, parasite (i.e. zero-lift) drag is enhanced as shown in Fig. 18 (b), probably due to structural members installed between the engines and the nacelle internal walls, which were not reflected in the wind-tunnel test model.

Fig. 14.   Preflight check on onboard avionics.

Fig. 15.   The prototype vehicle ascending just after takeoff.

Fig. 16.   The flight trajectory measured with onboard GPS receiver.
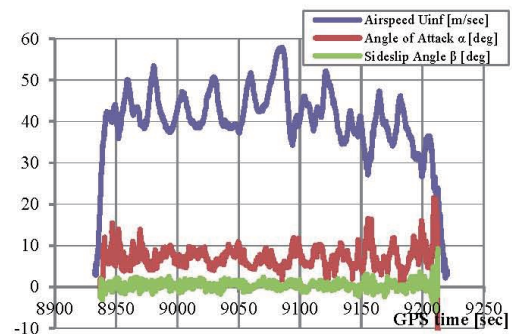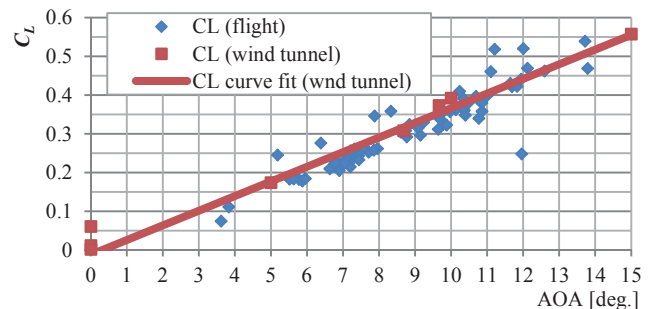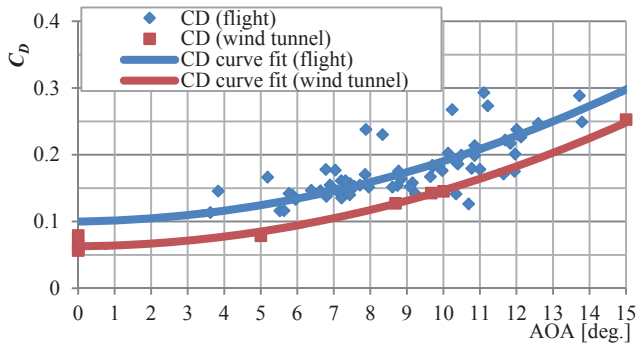

Fig. 17.   The airspeed and angles of attack and sideslip estimated from the ADS data.


(a) Lift coefficient versus angle of attack.

(b) Drag coefficient versus angle of attack.

Fig. 18. Aerodynamic coefficients estimated from the flight test in comparison with wind-tunnel test data rearranged for pitch-trim conditions.
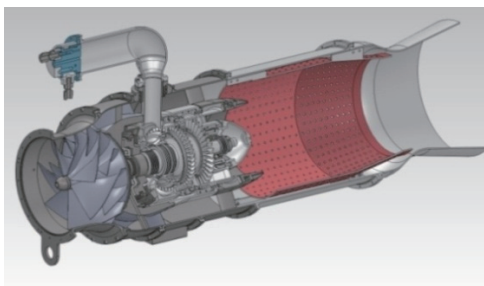
6. A Revised Configuration

6.1. A revision engine

An air-turbo ramjet gas-generator cycle (ATR-GG) engine is being designed for improvement in thrust at supersonic flights[10]. Its conceptual schematic is shown in Fig. 19 (a). Its turbine inlet condition is independent of the flight condition since the turbine is driven by the gas generator. Thus this type of engine is quite suitable to supersonic flights. The thrust and specific impulse of the proposed engine are rated at 3.8kN and 570sec respectively at a sea-level static condition, and 2.3kN and 720sec respectively at an altitude of 17km and Mach 2.0 (dynamic pressure 25kPa). The 3-D view of the proposed design is illustrated in Fig. 19 (b). Compressor fans and turbine bliscs were designed using the turbo-machinery design software AxCent and their fluid-dynamics were analyzed using the turbo-machinery analysis software FineTURBO as shown in Fig. 19 (c). The turbine bliscs, turbine nozzles and guide vanes of a prototype engine have been fabricated as shown partly in Fig. 19 (d). They are to be applied to ground rig tests in next year.
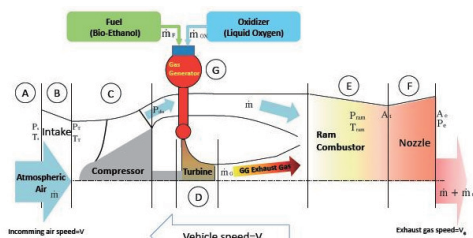
(a) A conceptual schematic.

(b) 3-D view of the engine design.
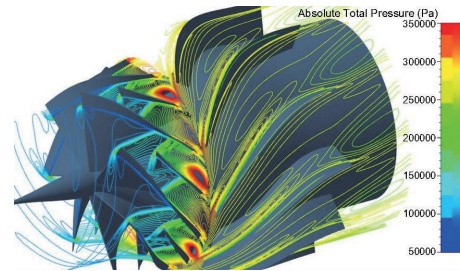
(c) CFD analysis of the compressor fans.

(d) A fabricated turbine blisc.

Fig. 19. The proposed ATR-GG engine.

6.2. A revised aerodynamic configuration

A revised aerodynamic configuration M2011 with a single ATR-GG engine is designed as shown in Fig. 20. Its wing and tail geometries are rigorously similar to those in the prototype vehicle; most of the aerodynamic data for the configuration M2006 and M2006prototype can be applied to the M2011. Its wingspan and fuselage diameter are enlarged by a factor of 1.5 so as to install an ATR-GG engine with a diameter of 230mm and to retain the ratio of wingspan to fuselage diameter. Three types of fuselage length, 5.8m, 6.8m, and 7.8m, are considered for various quantities of propellants loaded. In addition, three types of air-intake length are considered so as to allow uncertainty in intake design.

The longitudinal aerodynamics of the M2011 were measured by wind-tunnel tests as shown in Fig. 21. Its lift characteristics are quite similar to those for M2006 and M2006prototype, whereas the drag coefficient is reduced. Its pitching moment characteristics are adequate for all Mach numbers ranging from 0.3 to 2.0. In addition, the influence of the large nose length on the longitudinal aerodynamic is found to be small.
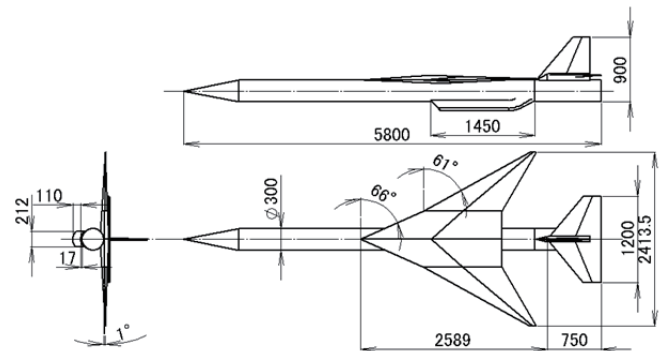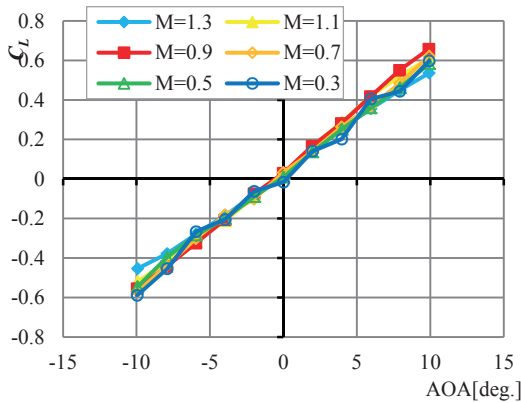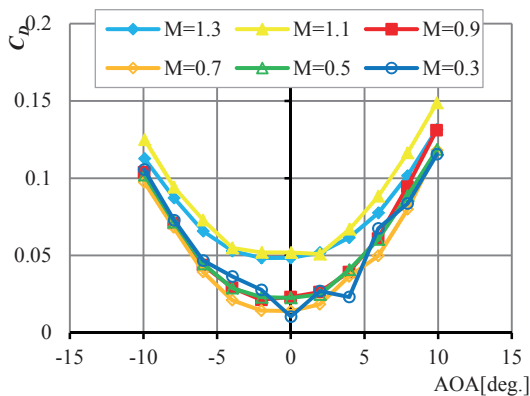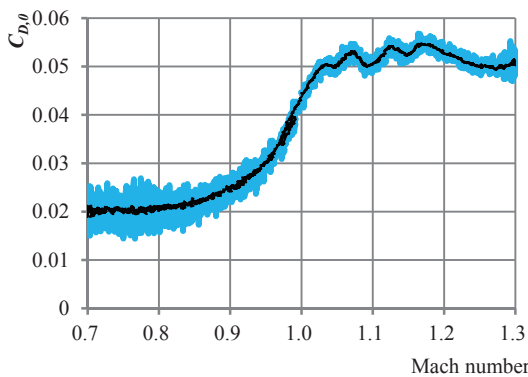

Fig. 20. The proposed revision configuration M2011.
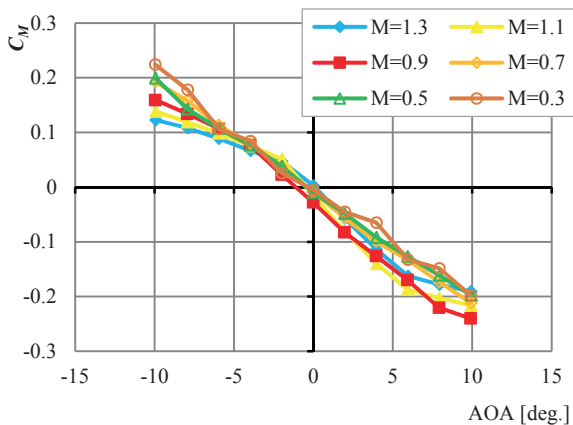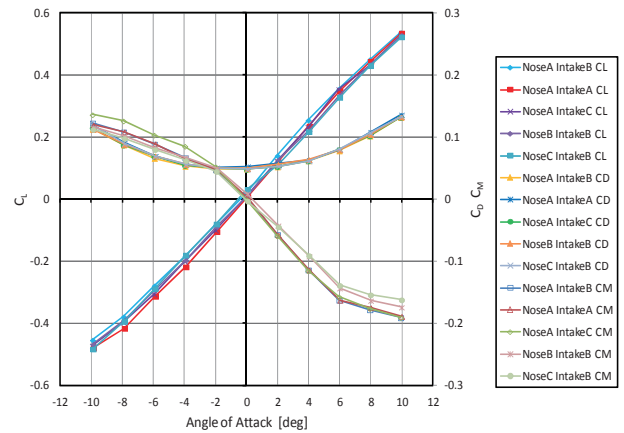
(a) Lift coefficient.

(b) Drag coefficient.

(c) Mach number dependence of the zero-lift drag coefficient.

(d) Pitching moment coefficient around the aerodynamic center of the main wing.

(e) Lift, drag, and pitching moment coefficients for several sets of nose and intake lengths at Mach 1.3.
Fig. 21. Longitudinal aerodynamics measured by wind tunnel tests for the configuration M2011.

6.3. Flight capability prediction

The thrust margin, i.e. thrust minus zero-lift drag, was evaluated for the present 2nd-generation vehicle with the aerodynamic configuration M2011 and an ATR-GG engine on the basis of the wind-tunnel tests and the engine design analysis. The results are illustrated in Fig. 22 with respect to flight Mach number and altitude. A green corridor is shown in the transonic region and a saddle point exists at about Mach 1.3 and 11km altitude. The vehicle must fly through this saddle point and the corridor in order to reach supersonic region.

Flight trajectory analysis of three degrees of freedom, i.e. point mass analysis, was carried out for several conditions on the engine rotation, the loaded propellant mass, and the reduction in drag and structural weight. One of the results is shown in Fig. 23, where an engine rotation of 105% and a loaded propellant of 130kg (correspondent to a fuselage length of 7.8m) were assumed. This result indicates a flight capability to reach Mach 2.0. Higher Mach numbers would be achieved by attaining reduction in overall drag and structural weight as well as by utilizing an acceleration assist such as the high-speed sled track facility[11].
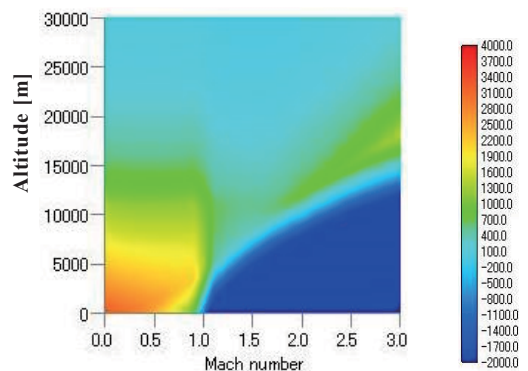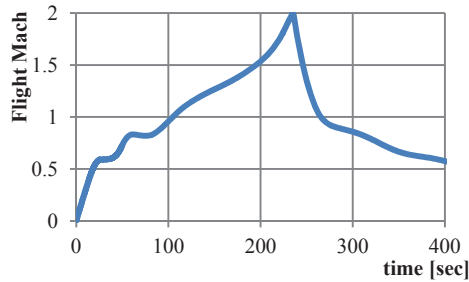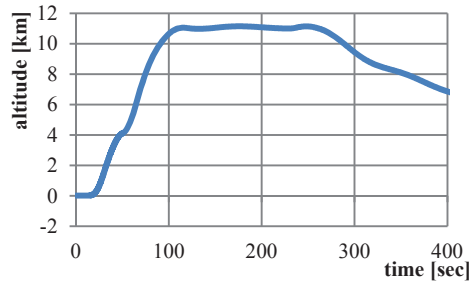

Fig. 22. Evaluated thrust margine for the 2nd generation vehicle.

(a)   History of the flight Mach number.

(b)   History of the flight altitude.

Fig. 23.   Results of the flight capability analysis of the 2nd generation vehicle with an ATR-GG engine. An engine rotation of 105% and a loaded propellant of 130kg are assumed.

7.   Conclusions

With the aims of creating and validating innovative fundamental technologies for high-speed atmospheric flights, a small scale supersonic flight experiment vehicle was designed as a flying test bed. Several aerodynamic configurations were proposed and analyzed by wind tunnel tests. A twin-engine configuration was selected as the baseline. Its flight capability was predicted by point mass analysis on the basis of aerodynamic characterization and propulsion performance estimation. In addition, a prototype vehicle with the almost equivalent configuration and dimension was designed and fabricated for verification of subsonic flight characteristics. Its first flight test was carried out in August 2010 and good flight capability was demonstrated. Furthermore a revised aerodynamic configuration and an air-turbo ramjet gas generator cycle (ATR-GG) engine are being designed for improvement in flight capability at higher Mach numbers. An autonomous guidance and control system will be designed on the basis of the acquired aerodynamics data. In addition, structure of the airframe will be revised, and the design of the proposed ATR-GG engine will be improved to fabricate actual engines for supersonic flights. Then the proposed supersonic flight experiment vehicle will be realized in near future. This prospective flight experiment vehicle will be applied to flight verification of innovative fundamental technologies for high-speed atmospheric flights such as turbo-ramjet propulsion with endothermic or biomass fuels, MEMS and morphing techniques for aerodynamic control, aero-servo-elastic technologies for efficient aerodynamic control with low-stiffness structure.

References

1) Kwak, D., Rinoie, K. and Kato, H.: Longitudinal Aerodynamics at High Alpha on Several Planforms of Cranked Arrow Wing Configuration, 2010 Asia-Pacific International Symposium on Aerospace Technology, Xian, China, September 13-15, 2010.
2) Kwak, D., Noguchi, M., Shirotake, M. and Rinoie, K.: Rolling Moment Characteristics of Supersonic Transport Configuration at High-Incidence Angles, Journal of Aircraft, **43** No. 4, pp.1112-1119, July–August (2006).
3) Kwak, D., Hirai, K., Rinoie, K. and Kato, H.: Rolling Moment Characteristics at High Alpha on Several Planforms of Cranked Arrow Wing Configuration, 27th AIAA Applied Aerodynamics Conference, 22-24 June 2009, San Antonio, Texas, USA.
4) Kwak, D., Shirotake, M. and Rinoie, K.: Vortex Behaviors over a Cranked Arrow Wing Configuration at High Angles of Attack, 24th International Congress of the Aeronautical Sciences, 29 August - 3 September 2004, Yokohama, Japan.
5) Hirai, K., Kwak, D. and Rinoie, K.: Vortex Behaviors of Cranked Arrow Wing Configurations with Different Wing Planforms, 26th International Congress of the Aeronautical Sciences, 14 - 19 September 2008, Anchorage, Alaska, USA.
6) Perkins, C. D. and Hage, R. E.: *Airplane Performance Stability and Control*, John Wiley & Sons, 1949.
7) Minato, R., Ota, T., Fukutomi, K., Tanatsugu, N., Mizobata, K., Kojima, T. and Kobayashi, H.: Development of Counter Rotating Axial Fan Turbojet Engine for Supersonic Unmanned Plane, Joint Propulsion Conference 2007, AIAA Paper 2007-5023, Cincinnati, USA.
8) Minato, R., Himeno, T., Kojima, T., Kobayashi, H., Taguchi, H., Sato, T., Arai, T., Mizobata, K., Sugiyama, H. and Tanatsugu, N.: Development of Counter Rotating Axial Fan Turbojet Engine for Supersonic Unmanned Plane at Muroran Institute of Technology, International Gas Turbine Congress, Tokyo, 2007.
9) Minato, R., Kato, D., Higashino, K. and Tanatsugu, N.: Development Study on Counter Rotating Fan Jet Engine for Supersonic Flight, ISABE 2011-1233, Goteborg, Sweden, 2011.
10) Minato, R., Higashino, K. and Tanatsugu, N.: Design and Performance Analysis of Bio-Ethanol Fueled GGcycle Air Turbo Ramjet Engine, AIAA Aerospace Science Meeting 2012, Nashville, Tennessee, USA, 2012.
11) Nakata, D., Yajima, J., Nishine, K., Higashino, K. and Tanatsugu, N.,: Research and Development of High Speed Test Track Facility in Japan, AIAA Aerospace Science Meeting 2012, Nashville, Tennessee, USA, January 2012.